MOLECULAR AND CELLULAR BIOLOGY, Oct. 1997, p. 5935–5945 Vol. 17, No. 10
0270-7306/97/$04.00+0


# Involvement of AP-2 in Regulation of the *R-FABP* Gene in the Developing Chick Retina

DWAYNE A. BISGROVE, ELIZABETH A. MONCKTON, AND ROSELINE GODBOUT*

*Department of Oncology, Cross Cancer Institute and University of Alberta, Edmonton, Alberta T6G 1Z2, Canada*

Received 25 February 1997/Returned for modification 31 March 1997/Accepted 29 July 1997

**Little is known regarding the molecular pathways that underlie the retinal maturation process. We are studying the regulation of the retinal fatty-acid-binding protein (*R-FABP*) gene, highly expressed in retinal precursor cells, to identify DNA regulatory elements and transcriptional factors involved in retinal development. Although the upstream sequence of the *R-FABP* gene is extremely GC rich, CpG methylation in this region is not implicated in the regulation of this gene because the 5′ flanking DNA remains unmethylated with tissue differentiation when there is a dramatic decrease in R-FABP transcript levels. Using a combination of DNase I hypersensitivity experiments, gel shift assays, and DNase I footprinting, we have found three sites of DNA-protein interaction within 205 bp of 5′ flanking DNA in the undifferentiated retina and four sites in the differentiated retina. DNA transfection analysis indicates that the first two footprints located within 150 bp of 5′ flanking DNA are required for high levels of transcription in primary undifferentiated retinal cultures. The first footprint includes a putative TATA box and Sp1 binding sites while the second footprint contains a consensus AP-2 DNA binding site. Supershift experiments using antibodies to AP-2 and methylation interference experiments indicate that an AP-2-like transcription factor present in both late-proliferative-stage retina and differentiated retina binds to the upstream region of the *R-FABP* gene. A combination of data including the expression profile of AP-2 during retinal development and DNA transfection analysis using constructs mutated at critical residues within the AP-2 binding site suggests that AP-2 is a repressor of *R-FABP* transcription.**

The fatty-acid-binding protein (FABP) family consists of a number of structurally related proteins with characteristic cellular, tissue, and developmental distribution patterns. Members of this family include heart FABP, intestinal FABP, adipocyte lipid-binding protein, myelin $P_2$, cellular retinoic-acid-binding proteins, and cellular retinol-binding proteins (1, 51). Some FABPs, such as adipocyte FABP and myelin $P_2$, are restricted to one tissue or organ type while others are more broadly expressed. For example, intestinal FABP is found in both intestine and stomach while liver FABP is present in liver, intestine, kidney, and stomach (reviewed in reference 51). Roles proposed for these proteins include the uptake, intracellular solubilization, storage, and/or delivery of fatty acids and retinoids (1). A role in signal transduction has also been proposed for heart FABP and adipocyte lipid-binding protein via phosphorylation of a tyrosine residue at position 19 by the insulin receptor (8, 41). Furthermore, mammary-derived growth inhibitor (also called heart FABP [46]) and liver FABP appear to be involved in the differentiation of mammary epithelial cells and in the control of hepatocyte cell proliferation, respectively (35, 36, 60). Some FABPs are located in both the nucleus and the cytoplasm, suggesting that they may play a role in carrying hydrophobic ligands to the nucleus (6, 7). Meunier-Durmort et al. (38) have recently shown that long-chain fatty acids are strong inducers of liver FABP gene expression.

The presence of a mammalian brain FABP was first reported in 1984 (2, 4), and the murine gene was cloned in 1994 (18, 37). The mouse brain FABP (B-FABP) has 67% amino acid identity with murine heart FABP and a lower level of homology with other members of the family (37). B-FABP expression correlates with neuronal differentiation in the mouse central nervous system, where the protein is primarily expressed in radial glial cells. Antibodies to B-FABP prevent both neuronal and glial cell differentiation of primary cerebellar cells in vitro. In these cultures, the extension of the radial glial processes is blocked as well as the migration of neuronal cells along the processes (18). Based on these observations, it was proposed that B-FABP is required for the establishment of the radial glial cell fiber system required for the migration of immature neurons in the developing nervous system. Using transgenic mice, Feng and Heintz (19) identified a radial glial cell-specific element located between 300 and 800 bp upstream of the *B-FABP* transcription initiation site.

We have identified an FABP transcript that is highly expressed in the retina and brain of the developing chicken embryo (24). The predicted amino acid sequence of retina FABP (R-FABP) is 85% identical to that of the mouse B-FABP. Homology to other members of the FABP family is considerably lower (e.g., 70% identity to bovine heart FABP, 59% to bovine myelin $P_2$, and 31% to rat intestinal FABP). Interestingly, B-FABP was not detected in the retina of the developing mouse embryo (37). We have found *R-FABP* to be highly expressed from day 3 (d3) (the earliest stage tested) to d7 in the chick retina as well as from d5 to d19 in the chick brain (24, 26), suggesting a role in chick retinal development-maturation in addition to the roles proposed for B-FABP in the brain.

Retinal development in the chick is divided into three overlapping stages: (i) cell proliferation and migration, which occurs primarily from d2 to d8 of incubation; (ii) readjustment to the proper layer (d8 to d10); and (iii) expression of differentiated properties (d11 to hatching at d21). At d3, the majority of cells in the chick retina are proliferating multipotential neuroectodermal cells that can differentiate into the six major classes of neuronal cells (photoreceptor, ganglion, bipolar, am-

* Corresponding author. Mailing address: Molecular Oncology Program, Cross Cancer Institute, 11560 University Ave., Edmonton, Alberta T6G 1Z2, Canada. Phone: (403) 432-8901. Fax: (403) 432-8892.

acrine, interplexiform, and horizontal) and one class of glial cells (Müller) that form the mature retina (49, 50, 53, 55, 56). At d7, 60% of the cells are proliferating, although the retina has differentiated to some extent and the innermost nerve fiber layer and ganglion cell layer are readily apparent (16, 44). By d9, only 10% of the cells are undergoing cell division (16). In the differentiated d19 retina, R-FABP mRNA levels are barely detectable, having undergone a 50- to 100-fold reduction compared to those at d3.5 (24, 26).

Here, we study the regulation of the *R-FABP* gene in order to gain insight into the molecular mechanisms that underlie retinal development. We have identified four DNA elements in the 5′ flanking region of the *R-FABP* gene that bind nuclear proteins. One of these elements contains a binding site for AP-2, a retinoic-acid-regulated transcriptional factor that plays an important role in the regulation of gene expression during mammalian embryogenesis.

## MATERIALS AND METHODS

**Primer extension analysis.** Poly(A)$^+$ RNA was isolated from d5 retina, d16 retina, and d16 heart as described previously (24). The 20-nucleotide (nt) primer 5′-GTTGTGGCTGTCCGCCAGCT-3′, corresponding to positions 38 to 57 bp of the R-FABP cDNA previously described (24), was end labelled with [$\gamma$-$^{32}$P]ATP (3,000 Ci/mmol) and T4 polynucleotide kinase. End-labelled primer was annealed to poly(A)$^+$ RNA at 42°C for 90 min, and the cDNA was extended at 50°C for 30 min with avian myeloblastosis virus reverse transcriptase, following the protocols supplied by Promega. Samples were run on an 8% polyacrylamide gel containing 7 M urea in 1× Tris-borate-EDTA (TBE) buffer. Marker lanes consisted of either labelled sequencing reaction mixtures or end-labelled $\phi$X174 phage digested with *Hin*fI.

**DNase I hypersensitivity analysis.** Procedures related to DNase I hypersensitivity experiments were as described elsewhere (27). Briefly, nuclei were isolated from 4 dozen d7 chick retinas by homogenization in cold 10 mM Tris-HCl (pH 7.5)–5 mM $MgCl_2$–0.5 M sucrose–0.15 mM spermine–0.5 mM spermidine and layering on a 0.88 M sucrose cushion in homogenization buffer. The nuclei were spun through the cushion at 5,000 rpm for 5 min in an HB-4 rotor. The nuclei were resuspended in 10 mM Tris-HCl (pH 7.5)–2.5 mM $MgCl_2$–0.25 M sucrose. DNase I (Worthington) was added to aliquots of nuclei to final concentrations of 0.1, 1, 2.5, 5, 10, and 25 μg/ml and incubated at 37°C for 10 min. An undigested control was included with each experiment. Digestion was stopped by adding 2 volumes of 10 mM Tris-HCl (pH 7.5)–1% sodium dodecyl sulfate (SDS)–5 mM EDTA–50-μg/ml proteinase K (Boehringer Mannheim). Samples were incubated overnight at 37°C, extracted with chloroform and phenol, and precipitated in ethanol. The purified DNAs (10 μg for each time point) were then digested with appropriate restriction enzymes and electrophoresed in a 1% agarose gel in 40 mM Tris-acetate–1 mM EDTA (pH 7.2). The DNA was transferred to nitrocellulose and hybridized with probes a, b, and c (described in the legend to Fig. 3) labelled by nick translation.

**DNA transfection analysis.** *R-FABP* 5′ flanking DNA fragments of different lengths were ligated to the 5′ end of the chloramphenicol acetyltransferase (CAT) gene in the pCAT basic vector (Promega): the −3.5-kb construct contains a 3,562-bp fragment from −3545 (*Ban*I) to +17 (*Ban*I), the −234-bp construct contains a 245-bp fragment from −234 (*Pvu*II) to +11 (*Rsa*I), the −135-bp construct contains a 145-bp fragment from −135 (*Sst*II) to +11 (*Rsa*I), and the −51-bp construct contains a 61-bp fragment from −51 (*Nae*I) to +11 (*Rsa*I). The −65-bp construct was obtained by ligating a PCR-generated fragment from −65 to +11 bp into the pCAT basic vector. To test the activity of the AP-2 binding site 5′-**GCC**GTG**GGC**-3′ (conserved residues in boldface), we generated two mutant constructs with base pair substitutions in the residues required for the binding of AP-2. In mutant 1, the AP-2 site (located at −75 to −67 bp) was mutated to GTTGTGGGC by PCR amplification of a DNA fragment spanning the AP-2 site using a primer containing the two mutated bases indicated by the underline, 5′-CGTTGTTGTGGGCGGCTCCCCTCCC-3′. In mutant 2, the AP-2 site was mutated to GTTGTGTTC with the following primer, 5′-CGTTG TTGTGTTCGGCTCCCCTCCC-3′, and mutant 1 DNA as the template DNA. Both mutant fragments were introduced into the −135-bp construct. All constructs were sequenced to ensure that only the intended mutations were introduced. Transient expression assays were as described by Graham and van der Eb (29) and Godbout et al. (25). To prepare primary retinal cultures, d5 retinas were dissected using an inverted microscope and digested with trypsin at 37°C for 5 min. The equivalent of three to four retinas/100-mm plate was cultured in Dulbecco modified Eagle medium plus 10% fetal calf serum. The cells were transfected when approximately one-third of the plate surface was covered (6 to 7 days after plating). For each transfection, 5 μg of CAT vector DNA and 5 μg of pSV-β-galactosidase control vector (internal control) (Promega) were precipitated in calcium phosphate and left on the cells for 16 h. The cells were harvested 48 to 50 h later. At this time, the plate was confluent or almost confluent. Cell extracts were prepared according to a freeze-thaw protocol provided by Promega, and CAT activity was measured with [$^{14}$C]chloramphenicol in the presence of *n*-butyryl coenzyme A. Samples were assayed by both liquid scintillation counting and thin-layer chromatography. β-Galactosidase activity was measured in 96-well plates with a plate reader (405 nm) and ONPG (*o*-nitrophenyl-β-D-galactopyranoside) as the substrate. As an additional control for transfection efficiency, Hirt DNA was prepared and analyzed by Southern blotting with CAT vector DNA as the probe (31).

**CpG methylation analysis.** Genomic DNA was prepared as described by Sambrook et al. (45). Cytosine deamination by bisulfite treatment and PCR amplification was performed according to the method of Frommer et al. (20) as modified by Clark et al. (13). Briefly, 10 μg of genomic DNA from d5 chick retina, d16 chick retina, and adult chicken liver was digested with *Bam*HI, denatured with sodium hydroxide, and treated with sodium bisulfite and hydroquinone for 16 h at 55°C. The free bisulfite was removed with a desalting column (Promega Magic DNA Clean-Up System). The DNA was treated with sodium hydroxide, neutralized with ammonium acetate, ethanol precipitated, and resuspended in 100 μl of TE (10 mM Tris-HCl [pH 7.5], 1 mM EDTA). PCR amplification was carried out with *Taq*I polymerase (Stratagene) and the following primers: primer 1, 5′-TAAAGTTGTGGTTGTT(T/C)GTTAG-3′, from positions +60 to +81 where (T/C) represents the location of a C that could potentially be methylated; and primer 2, 5′-CACTAAAAATTACCTTCACTTA ACC-3′, from positions −442 to −418. The PCR products were reamplified with a nested primer (primer 3) from positions −355 to −335 (5′-CTCCCAAAAACC TTATCCTAC-3′) and with primer 1. The amplified DNA was ligated into pBluescript with a T overhang (33) and transformed into XL1-Blue. DNA inserts were sequenced with T7 DNA polymerase (Pharmacia) and the M13 forward and reverse primers.

**DNA-protein binding assays.** Nuclear extracts were prepared from d7 retina and d16 retina as previously described (28, 52). Protein concentrations were measured by the Bradford assay (Bio-Rad).

**(i) Footprinting analysis.** The 245-bp *Pvu*II/*Rsa*I *R-FABP* genomic DNA fragment from −234 to +11 bp was ligated into the *Sma*I site of the pBluescript vector. The top and bottom strands were separately labelled by digesting the construct with either *Xba*I or *Hin*dIII, filling in with Klenow polymerase and [$^{32}$P]dCTP, and cutting out the insert with either *Hin*dIII or *Xba*I. The labelled DNAs were purified on a polyacrylamide gel. Procedures related to DNase I footprinting analysis were as described previously except that no polyvinyl alcohol was added (34). Briefly, 10 fmol of DNA was combined with 10 to 20 μg of nuclear extract and incubated in 50 μl of binding buffer containing 0.25 μg of poly(dI-dC) for 15 min on ice, followed by 2 min at room temperature. An equal volume of start buffer containing 5 mM $CaCl_2$ and 10 mM $MgCl_2$ was added, and the mixture was digested with 4 to 6 μl of a 5-μg/ml solution of DNase I (Worthington). The reaction was stopped after 1 min. Samples were purified by phenol-chloroform extraction and ethanol precipitation and resolved on a 7% polyacrylamide sequencing gel. As a negative control, the DNA without nuclear extract was digested with DNase I. The G+A sequencing ladder was prepared according to the method of Belikov and Wieslander (3).

**(ii) Electrophoretic mobility shift assay (EMSA).** The *Nae*I/*Eag*I fragment from −52 to −90 bp (containing footprint II) was labelled by filling in at the *Eag*I site with Klenow polymerase. EMSAs were performed with 0.025 pmol of labelled DNA in a final volume of 20 μl containing 2 μg of poly(dI-dC) and 15 μg of nuclear extract (42). The following DNA fragments (100× molar excess) were used as competitors: the *Eag*I/*Nae*I fragment from −9 to −51 bp that includes footprint I; the −52- to −90-bp *Nae*I/*Eag*I fragment that includes footprint II; and three double-stranded consensus oligonucleotides to the Sp1, AP-2, and CTF/NF1 transcription factors (Promega). The −52- to −90-bp *Nae*I/*Eag*I fragment containing the two base pair substitutions in the AP-2 site (described as mutant 1 in the DNA transfection section) was tested for its ability to bind nuclear proteins under the same conditions as for the wild-type (WT) *Nae*I/*Eag*I fragment. For the supershift experiments, we used 2 μl of either anti-human AP-2 antibody (Santa Cruz Biotechnology) or anti-human TFIID (TATA-box-binding protein [TBP]) antibody (Promega) following the protocol supplied by Santa Cruz Biotechnology. Anti-human NF1 antibody (Santa Cruz Biotechnology) was also used in some experiments.

**(iii) Methylation interference assay.** The noncoding strand of the −52- to −90-bp *Nae*I/*Eag*I DNA fragment and the coding strand of the −9- to −90-bp *Eag*I/*Eag*I DNA fragment were individually end labelled with [$^{32}$P]dCTP with Klenow polymerase. The labelled DNA fragments were partially methylated at G and A residues with dimethyl sulfate as described elsewhere (21). Binding reactions were carried out as described for the EMSA with a fivefold scale-up. Free and bound molecules were separated on an 0.5× TBE–6% polyacrylamide gel, eluted from the gel slices by a soaking in 0.2 M NaCl–20 mM EDTA (pH 8.0)–1% SDS–1-mg/ml tRNA, and cleaved in 10% piperidine at 90°C for 30 min. Residual piperidine was removed by lyophilization. The cleavage products were analyzed on either an 8% or a 12% denaturing polyacrylamide gel.

**Northern and Western blot analyses.** Poly(A)$^+$ RNA was isolated from d5, d7, d10, and d16 retinas as described earlier (24). The RNA was transferred to a nitrocellulose filter, hybridized to a 1.5-kb AP-2 cDNA isolated from a human adult retina cDNA library (Genome Systems Inc.; clone 362684; accession no. AA018570 and AA018571), and washed at 45°C in 0.1× SSC (1× SSC is 0.15 M NaCl plus 0.015 M sodium citrate) and 0.1% SDS. The ends of the AP-2 cDNA

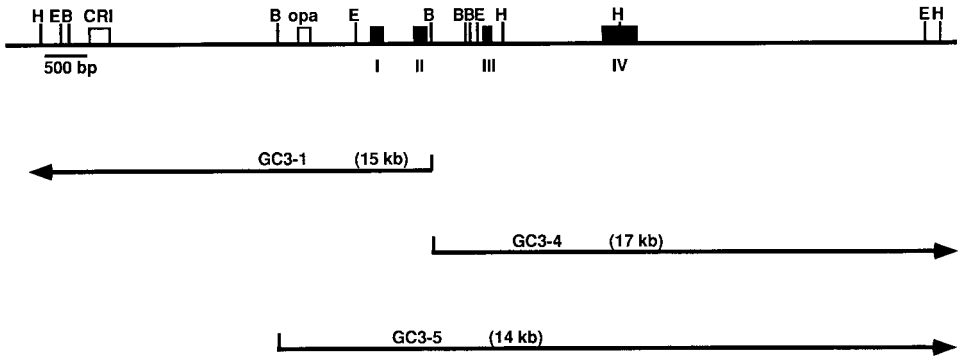


FIG. 1. Map of the *R-FABP* gene. The three bacteriophages GC3-1, GC3-4, and GC3-5 were selected by screening a chicken genomic library with R-FABP cDNA. The size of the genomic DNA insert is indicated in parentheses. The four exons are represented by black boxes, while the open boxes represent the location of CRI and Opa repetitive elements. Sites recognized by the following restriction enzymes are indicated: *Hin*dIII (H), *Eco*RI (E), and *Bam*HI (B).

were sequenced to ensure that it was the correct clone. The filter was hybridized to mouse α-actin cDNA to control for lane-to-lane variation in RNA levels.

To analyze levels of AP-2 in nuclear extracts, proteins were electrophoresed in an 8% polyacrylamide–SDS gel and electroblotted onto nitrocellulose. The filter was incubated with a 1:1,000 dilution of anti-human AP-2 antibody (Santa Cruz Biotechnology). Antigen-antibody interactions were visualized with the ECL Western blotting analysis system (Amersham) with a 1:100,000 dilution of peroxidase-linked secondary anti-rabbit immunoglobulin G antibody (Jackson ImmunoResearch Laboratories).

## RESULTS

**Structure of the *R-FABP* gene.** The 709-bp R-FABP cDNA isolated from a d3.5 chick retina cDNA library was used to probe a chicken genomic library. Three independent bacteriophages were isolated: GC3-1, with an insert of ~15 kb; GC3-4, with an insert of ~17 kb; and GC3-5, with an insert of ~14 kb. Restriction enzyme digestions and partial sequence analyses of the inserts contained in these three bacteriophages generated the physical map shown in Fig. 1. The *R-FABP* gene is contained entirely within a 3.5-kb DNA fragment. GC3-1 contains ~14 kb of 5′ flanking DNA while GC3-4 contains ~14 kb of 3′ flanking DNA. A middle repetitive sequence element, CR1, is located ~4 kb upstream of the *R-FABP* gene. Another repetitive element, Opa, is located ~1 kb upstream of the gene. Opa repeats are sometimes translated, forming long tracts of polyglutamine (54). Northern blot analysis of poly(A)$^+$ RNAs isolated from chick tissues (including retina) with a DNA fragment containing the Opa repetitive element as the probe suggest that this Opa repeat is not transcribed in the chick (data not shown).

The structure of the chick *R-FABP* gene is similar to that reported for mammalian *FABP* genes with exons 1 to 4 encoding amino acids (aa) 1 to 24, aa 25 to 82, aa 83 to 116, and aa 117 to 132, respectively. The fourth exon is the longest, consisting of 352 bp, 301 bp of which represents the 3′ untranslated region. Donor and acceptor splice sites conform to the GT/AG rule.

**Identification of the 5′ end of the R-FABP transcript.** The R-FABP cDNA isolated from a chick retina library contains 9 bp of 5′ untranslated sequence. To determine the exact site of transcription initiation, primer extension analysis was carried out with a 20-nt oligomer corresponding to positions 38 to 57 of the cDNA described earlier (24). Poly(A)$^+$ RNA was isolated from d5 retina and d16 brain, both of which express elevated levels of R-FABP transcript, and from d16 heart, which expresses no (or undetectable) R-FABP mRNA. Extended products of ~75 nt were observed in the d5 retina and d16 brain but not in the d16 heart (Fig. 2A). To determine the exact site of transcription initiation, the same reaction mixtures were run on an 8% denaturing polyacrylamide gel alongside previously analyzed sequencing reactions. Three major extended products of 75, 76, and 77 nt were identified. The transcription initiation sites of R-FABP mRNA are therefore located 18 to 20 nt upstream of the 5′ end of the longest cDNA isolated from the chick retina library (Fig. 2B). The 5′-most nucleotide is designated +1.

A putative TATA box is located 30 bp upstream of the transcription initiation site. However, as shown in Fig. 2B, the classic TATAAA sequence is replaced by TTTAAA in the *R-FABP* gene. In 97% of TATA boxes, an "A" is found in the second position. A "T" in this position has been reported in only 2% of TATA box-containing genes. It is therefore not clear whether this sequence represents a bona fide TATA box. A notable feature of the sequence immediately upstream of the transcription initiation site is its extremely high GC content. Over a 200-bp sequence, 162 bp (81%) are G's or C's. These are indicated in boldface in Fig. 2B.

**Localization of DNase I-hypersensitive (HS) sites flanking the *R-FABP* gene.** An efficient way to scan relatively large regions of DNA for the presence of regulatory elements is to treat nuclei with increasing concentrations of DNase I and to analyze the digested DNA by Southern blotting. This technique has been used to identify both proximal and distal regulatory elements in a large number of genes (30, 48, 59). Nuclei from d7 chick retina cells were digested with 0.1, 1, 2.5, 5, 10, and 25 μg of DNase I per ml. Genomic DNA was isolated from each nuclear preparation, digested with *Hin*dIII, run on a 1% agarose gel, and transferred to nitrocellulose. Duplicate blots were hybridized with a 500-bp *Hin*dIII/*Bgl*I DNA fragment (probe a) from the 5′ end of the *R-FABP* gene (Fig. 1 and 3A and C) and with a 500-bp *Sca*I/*Xho*I fragment (probe b) located between exons 1 and 2 (Fig. 3B and C). With probe a, the expected 6-kb fragment representing intact genomic DNA was obtained as well as a ~4.2-kb fragment that increased in intensity with increasing DNase I concentration. Probe b hybridized to the intact 6-kb genomic DNA fragment as well as to a ~1.8-kb fragment that increased in intensity in a DNase I-dependent manner. Both HS sites correspond to the same location at the 5′ end of the *R-FABP* gene, immediately upstream of the transcription initiation site in the GC-rich region shown in Fig. 2. This site is indicated by a large asterisk in Fig. 3. A weak HS site at ~4.4 kb was also detected when the filter was hybridized with probe b. This HS site is indicated by the small asterisk in Fig. 3. Since this HS site was found in only one orientation and was very weak, it was not analyzed further.

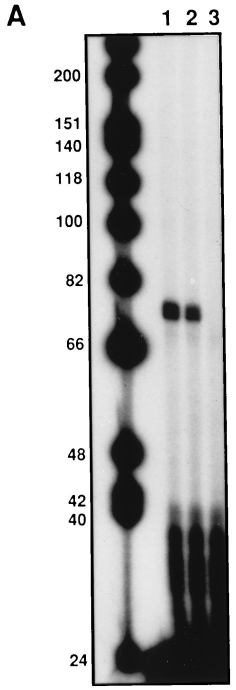


B

```
                                                    TGATGCCGCCCCGCGAGCGC     -200
CCCAACACCGCCGGCCCCCACCAATCCCCGCGCAGCGCGGTTGGCCGCGGGGCGGTGAGAG           -180
CCCTCCCGGCGGGGCGGGCAGACTCCGGCCGCCGTCCCGCCCGTTGCCGTGGGCGGCTCC            -120
CCTCCCGCCGGCCCCCCGCCGGGCGCGGGCTTTAAATGCGGGGCGGTGAGGCGGCCGTGG             -60

***
CGTTTCCCCGTACTCCGGCACCCGCTGCCATGGTTGAGGCTTTCTGCGCGACGTGGAAGC              +1
TGGCGGACAGCCACAACTTTGACGAATACATGAAGGCGCTGG                               +61
```

FIG. 2. Identification of the 5′ end of the R-FABP transcript. (A) Primer extension analysis was carried out with a 20-nt primer (5′-GTTGTGGCTGTC CGCCAGCT-3′) corresponding to positions 38 to 57 of the R-FABP cDNA described in the work of Godbout (24). Poly(A)$^+$ RNAs from d5 retina (lane 1), d16 brain (lane 2), and d16 heart (lane 3) were incubated with the 5′-end-labelled antisense primer, and the cDNA was extended with reverse transcriptase. The cDNA fragments were resolved on an 8% denaturing polyacrylamide gel. Size markers (in nucleotides) are indicated on the side. The band at ~75 nt represents the longest cDNA product and is specific to the tissues that express R-FABP mRNA. (B) Partial sequence of *R-FABP* gene in the vicinity of the transcription initiation site. The start methionine codon is underlined, and the three sites of transcription initiation are indicated by the asterisks. The G's and C's in the 200-bp 5′ flanking DNA are in boldface.

Regulatory elements have been found not only in the 5′ flanking region of genes but also within genes and in their 3′ flanking regions. We therefore analyzed the downstream region of the *R-FABP* gene for the presence of HS sites. The DNase I-treated genomic DNA was digested with *Eco*RI, generating a 6-kb fragment that includes exons 3 and 4 as well as 3.5 kb of 3′ flanking DNA. Using a 250-bp *Eco*RI/*Hin*dIII fragment as the probe (labelled "c" in Fig. 3C), we obtained a strong band at 6 kb but no additional smaller bands that would indicate the presence of HS sites. The strong HS site located at the 5′ end of the *R-FABP* gene suggests that a major regulatory domain(s) is located immediatedly upstream of the transcription initiation site.

**Methylation analysis of the R-FABP promoter.** DNA methylation in promoter regions has been implicated in the regulation of cell-, tissue-, and development-specific genes (17). In general, hypomethylation of CpG residues correlates with gene expression while hypermethylation correlates with nonexpression. The 5′ end of the *R-FABP* gene is exceedingly GC rich, with 33 CpG dinucleotides within 200 bp of 5′ flanking DNA. A recently developed method (13, 20) allows the analysis of the methylation status of every C residue. We have used this technique to analyze the methylation state of the region from −334 to +59 bp in preparations of genomic DNA from d5 retina (elevated levels of R-FABP mRNA), d16 retina (low levels of R-FABP mRNA), and adult chicken liver (no detectable R-FABP mRNA by Northern blot analysis). The bisulfite-treated DNAs were PCR amplified first with primers 1 and 2 and subsequently with primer 1 and the nested primer 3 as described in Materials and Methods. Because of the reported variability in methylation patterns observed by others (40), we sequenced both strands of six independent clones from each of the genomic DNAs. Surprisingly, all of the C's in all of the DNAs sequenced were converted to T's, indicating that none of the C residues in this region was protected by methylation (data not shown). As a result of bisulfite treatment, the two strands of DNA contain many base substitutions which result in considerable difference in the sequence of one strand relative to the other. The three-primer PCR strategy described here will therefore amplify only the strand of DNA to which the primers were made. We did not sequence the other DNA strand because there is no evidence that methylation can occur on only one strand. Based on these data, we conclude that methylation in the immediate upstream region of the *R-FABP* gene is not involved in either the dramatic reduction in R-FABP transcript levels observed from d5 to d16 in the chick embryo or the repression of *R-FABP* gene activity in adult liver.

**Analysis of regulatory domains by DNA transfection of primary retinal cultures.** We transfected primary chick retinal cultures from d5 embryos to determine whether the 5′ flanking region of the *R-FABP* gene has regulatory activity. Four different constructs were tested; either 51 bp, 135 bp, 234 bp, or 3.5 kb of 5′ flanking DNA was linked to the CAT reporter gene and introduced into primary cultures of retinal cells by calcium phosphate-mediated DNA transfection. A CAT vector (pCAT basic) containing no enhancer and no promoter served as the negative control. The results of four separate experiments are individually tabulated in Fig. 4A. Each number presented in this figure is an average of at least two separate measurements of CAT activity. β-Galactosidase activity was measured in each case to ensure that the transfection efficiencies were similar for each plate. There was less than a twofold variation in β-galactosidase activity from sample to sample within each set of experiments. Because we used primary cultures, there was more variation in CAT activity from experiment to experiment than ordinarily observed with established cultures. However, a similar trend was observed in all four experiments: CAT activity increased 8- to 25-fold in constructs containing 51 bp of *R-FABP* upstream sequence compared to pCAT basic. An additional ~4- to 5-fold increase was obtained with 135 bp of upstream sequence. Little or no further increase in CAT activity was observed with the −234-bp construct while the −3.5-kb construct consistently generated lower CAT activity than either the −135- or −234-bp constructs, suggesting that the sequence from −234 bp and −3.5 kb has a negative influence on transcription. To ensure that the −3.5-kb construct was taken in by the cells as efficiently as the other constructs, we measured levels of transfected plasmid DNAs by the method of Hirt (31). There was less than a twofold variation from construct to construct (data not shown). These data suggest that sequences located within 135 bp of 5′ flanking DNA

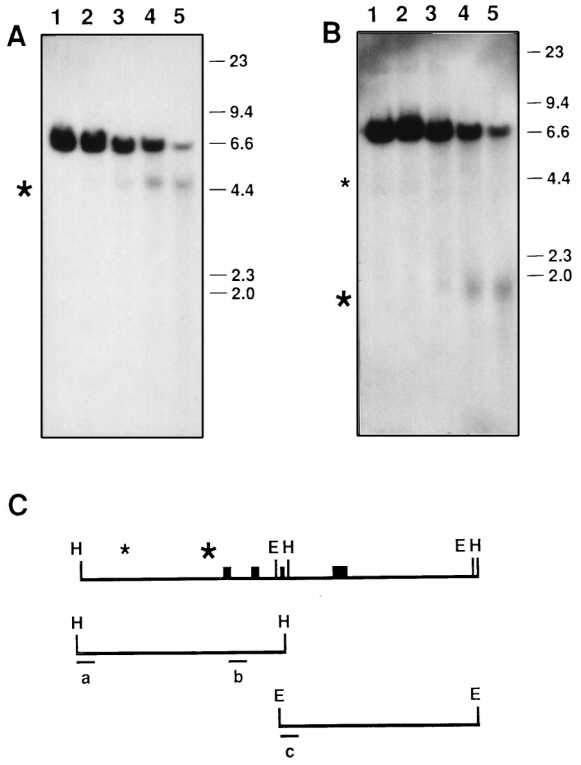


FIG. 3. DNase I hypersensitivity of the *R-FABP* gene. (A and B) Nuclei from d7 chick retina were treated with increasing concentrations of DNase I (lanes 1, no DNase I; lanes 2, 0.1 μg/ml; lanes 3, 1 μg/ml; lanes 4, 5 μg/ml; lanes 5, 10 μg/ml). The DNA was extracted from each sample and digested with *Hin*dIII. The DNA was transferred to nitrocellulose filters and hybridized with a 500-bp *Hin*dIII/*Bgl*I fragment from the 5′ end of the *R-FABP* gene (probe a) (A) and a 500-bp *Sca*I/*Xho*I fragment located between exons 1 and 2 (probe b) (B) (the *Xho*I site is derived from the phage polylinker region). The HS sites are indicated by the asterisks. Size markers in kilobase pairs are indicated at the right. (C) Diagrammatic representation of the *R-FABP* gene indicating the location of the probes (fragments a, b, and c) used for hybridization. Results obtained with fragment c are described in the text. Restriction enzymes are *Hin*dIII (H) and *Eco*RI (E).

are especially important for the upregulation of the *R-FABP* gene.

**DNA-protein interaction analysis of the *R-FABP* promoter.** Transient DNA transfection of primary retinal cultures using the CAT assay suggests that full activity is obtained with the −234-bp construct and that most of the activity is within 135 bp of 5′ flanking DNA. To analyze the sites of protein-DNA interaction within this region, in vitro DNase I footprinting analysis was carried out with a *Pvu*II/*Rsa*I genomic DNA fragment from −234 to +11 bp. To compare sites of DNA-protein interaction in the undifferentiated versus differentiated retina, nuclear extracts were prepared from d7 retina and d16 retina. Regions protected from DNase I digestion are shown in Fig. 5. When the coding strand was labelled, four distinct footprints were observed in the d16 retinal extracts: from −24 to −52 bp (footprint I), −59 to −80 bp (footprint II), −114 to −140 bp (footprint III), and −199 to −205 bp (footprint IV). The patterns obtained with d7 retina were similar except that footprint II extended only from −63 to −80 bp and footprint III was not detected in these extracts although there was a DNase I HS site at position −129. DNase I footprinting of the noncoding strand consistently produced footprints that were less clear than those observed on the coding strand. A number of strong bands in the region from −85 to −145 showed a reduction in intensity although extended areas of reduced intensity corresponding to footprints were not obvious. The following footprints were obtained on the noncoding strand with d16 retinal extracts: from −206 to −195 bp (footprint IV), −143 to −122 bp (footprint III), −63 to −80 bp (footprint II), and −52 to −27 bp (footprint I). Footprints I, II, and IV were also observed with d7 retinal extracts. There is therefore a general agreement with the footprints on the coding and noncoding strands.

As mentioned earlier, the 5′ flanking region of *R-FABP* is extremely GC rich (Fig. 2B). The sequence protected in footprint I consists of a stretch of G's and C's followed by the putative TATA (TTTAAA) box (Fig. 6). A number of possible Sp1 binding sites are located within this region. Similarly, footprints II and III consist almost entirely of G's and C's, while the nucleotides protected by footprint IV are 5′-GATAAT-3′ (Fig. 6). Interestingly, there is an AP-2 consensus binding site within footprint II—5′-**GCC**GTG**GGC**-3′ (the conserved residues are indicated in boldface). Footprint II is located within the 135-bp 5′ flanking DNA of the *R-FABP* gene that generates a high level of activity in the DNA transfection

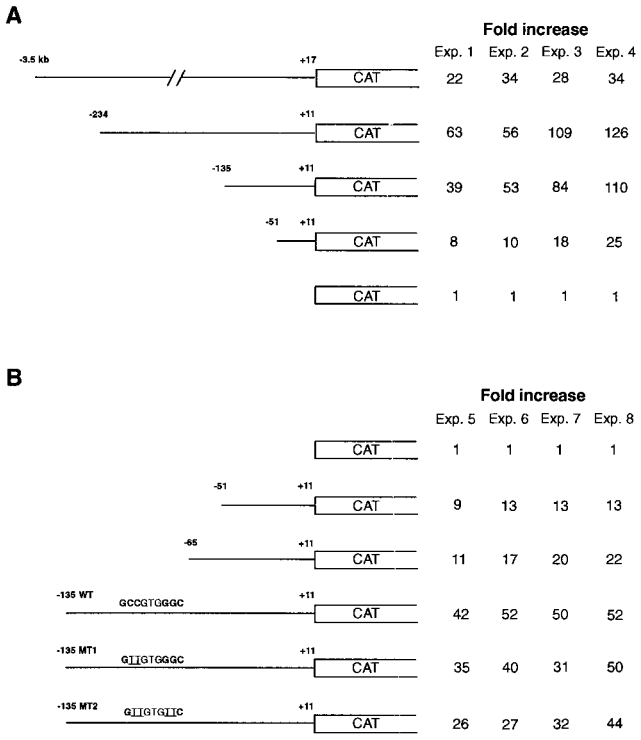


FIG. 4. Analysis of the regulatory activity of the *R-FABP* 5′ upstream region by the CAT assay. (A) Four DNA fragments containing from −3.5 kb to +17 bp, −234 to +11 bp, −135 to +11 bp, and −51 to +11 bp were ligated to the pCAT basic vector containing no promoter or enhancer. Primary d5 retinal cultures were transfected, and CAT activity was measured by the conversion of [$^{14}$C] chloramphenicol to its butyrylated derivatives. The results from four separate experiments are tabulated. Each number represents the average fold increase in CAT activity for each construct compared to pCAT basic. Numbers have been adjusted to account for construct size and for variations in β-galactosidase activity. (B) WT and mutant (MT) AP-2 recognition sites in the context of the −135-bp construct described above were transfected into primary d5 retinal cultures. In −135 MT1, the AP-2 site (GCCGTGGGC) was mutated to GTT-GTGGGC, and in −135 MT2, the AP-2 site was mutated to GTTGTGTTC. The −65-bp construct was prepared by PCR amplification of the region from −65 to +11 bp. The fold increases indicated for experiments 5 to 8 have been adjusted for variations in levels of transfected DNA by densitometric scanning of gels containing Hirt DNA.

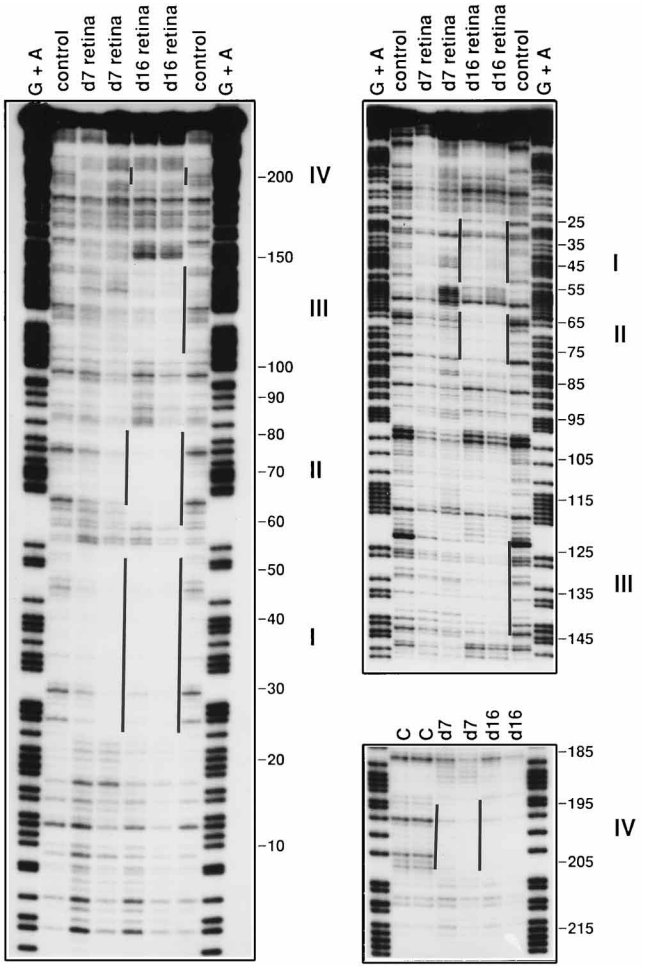


FIG. 5. DNase I footprinting of the protein binding sites in the *R-FABP* promoter region. The top and bottom strands of the 245-bp *Pvu*II/*Rsa*I *R-FABP* DNA fragment from −234 to +11 bp were separately labelled, incubated with nuclear extracts prepared from either d7 retina or d16 retina (15 μg of nuclear extracts), digested with either 0.2 (lanes 3 and 5) or 0.3 (lanes 4 and 6) μg of DNase I per ml, and run on a 7% denaturing polyacrylamide gel. The samples were loaded in a different order in the bottom right gel, with 0.2-μg/ml DNase I in lanes 4 and 6 and 0.3-μg/ml DNase I in lanes 5 and 7. The results obtained with the coding strand are shown on the left, and those with the noncoding strand are shown on the right. G+A lanes represent the purine sequence of the radiolabelled coding (left) and noncoding (right) strands. Numbers on the right refer to positions relative to the transcription initiation site (designated as +1). Control lanes consist of protein-free DNA cut with DNase I. Footprints I to IV are indicated by the lines on the right-hand side of lanes 4 (d7 retina) and 6 (d16 retina) of the gels located on the left and top right. Footprint IV on the bottom right gel is indicated on the left of lanes 4 (d7 retina) and 6 (d16 retina).

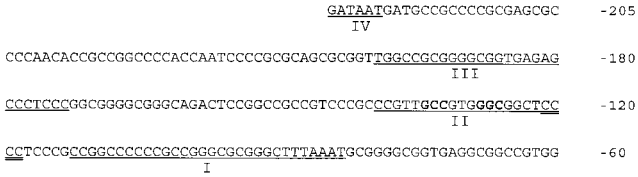


FIG. 6. Location of the footprints in the *R-FABP* upstream sequence. The 205-bp sequence located upstream of the transcription initiation site is indicated as well as the location of the footprints (single underline) found within this region with d7 and d16 retinal extracts. The double underline represents the extended footprint II observed with d16 retinal extracts. Footprint III is observed only with d16 retinal extracts. The conserved nucleotides in the AP-2 binding site are indicated in boldface.

analysis. To further analyze footprint II, EMSA was carried out with a labelled DNA fragment from −52 to −90 bp as the probe. A similar pattern was obtained with both d7 and d16 retinal extracts although the intensity of the bands observed with d7 extracts was consistently weaker than that observed with d16 extracts (Fig. 7). In the absence of specific competitors, a strong retarded band (indicated by the arrow) and multiple weaker retarded bands were observed (lanes 1 and 6 in Fig. 7). When the −52- to −90-bp DNA fragment was used as a competitor, these bands either disappeared or were substantially reduced in intensity, including the strong band indicated by the arrow (lanes 2 and 7). With a DNA fragment from −9 to −51 bp as the competitor, there was only a slight decrease in the intensity of the bands (lane 11). In the presence of a 100× excess of consensus double-stranded oligonucleotides to SP1, AP-2, and CTF/NF1, competition was observed only in the lanes containing the AP-2 oligonucleotide (lanes 4 and 9), where two of the retarded bands either disappeared or were significantly reduced in intensity (including the band indicated by the arrow). The remaining bands were not affected by the presence of excess unlabelled AP-2 oligonucleotide. To obtain additional evidence that an AP-2-like transcription factor is binding to the −52- to −90-bp region, nuclear extracts from both d7 and d16 retinas were incubated with either an antibody to AP-2 or an antibody to TBP prior to addition of the labelled −52- to −90-bp DNA fragment. As shown in Fig. 8, a supershifted band was observed in the presence of the AP-2 antibody. Supershifting was not obtained in the presence of either TBP antibody (shown) or NF1 antibody (not shown).

We used the methylation interference assay to determine which purine residues in the −52- to −90-bp region are in

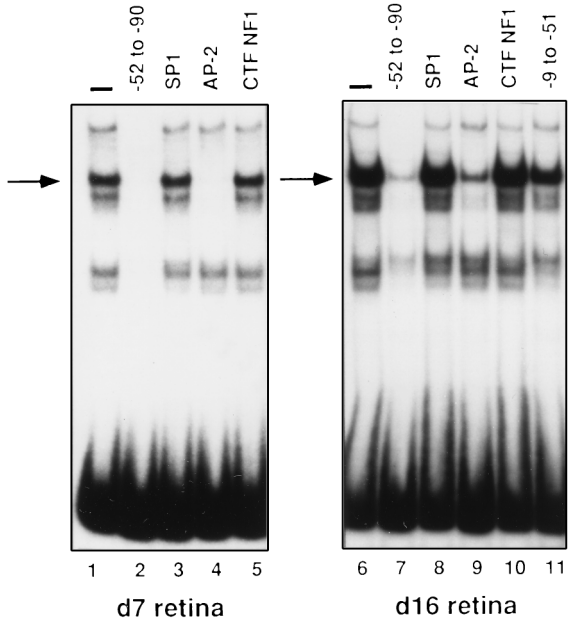


FIG. 7. EMSA with a DNA fragment (−52 to −90 bp) containing footprint II as the probe. The $^{32}$P-labelled probe (−52 to −90 bp) was incubated with nuclear extracts from either d7 or d16 retina and run on a 6% nondenaturing polyacrylamide gel in 0.5× TBE. The following competitors (in ~100× molar excess) were tested: no competitor (lanes 1 and 6), unlabelled −52- to −90-bp DNA fragment (lanes 2 and 7), SP1 oligonucleotide (lanes 3 and 8), AP-2 oligonucleotide (lanes 4 and 9), CTF/NF1 oligonucleotide (lanes 5 and 10), and −9- to −51-bp DNA fragment (lane 11). The arrows indicate the location of the strongest specific DNA-protein band. The free probe is at the bottom of the gel.

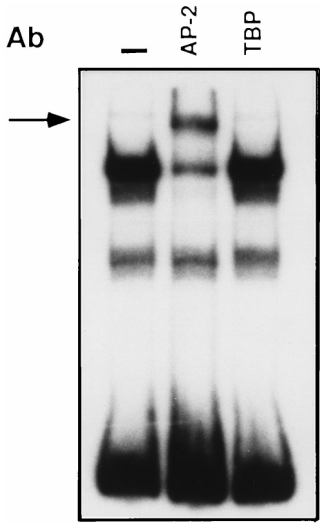


FIG. 8. Supershift of a DNA-protein band with the AP-2 antibody. EMSA was carried out with the $^{32}$P-labelled DNA fragment from −52 to −90 bp and either d7 (not shown) or d16 (shown) retinal extract in the presence of AP-2 antibody or TBP antibody. A supershifted band indicated by the arrow was observed in the presence of the AP-2 antibody. Ab, antibody.

close proximity to the transcription factor found in the major EMSA band. Figure 9 shows that methylation of G residues at positions −74, −73, and −67 on the noncoding strand and −75, −72, −70, −69, and −68 on the coding strand interferes with protein binding. This pattern was identical for both d7 and d16 retinal extracts. Methylation of a G (indicated by the arrow) located outside the AP-2 binding site at position −64 on the noncoding strand also interfered with protein binding. Similar methylation interference patterns were observed for the AP-2 DNA binding sites in the simian virus 40 enhancer and human metallothionein IIa distal basal-level element, except that no extension beyond the AP-2 site was noted (57).

**AP-2 expression in the retina.** The DNA transfection results indicate that footprint II, which includes the AP-2 binding site, plays a positive role in the regulation of the *R-FABP* gene. However, the DNA-protein interaction experiments suggest that AP-2 is more abundant (or more active) in the differentiated d16 retina (which expresses low levels of R-FABP mRNA) than in d7 retina (which has elevated levels of R-FABP mRNA). An AP-2α cDNA isolated from a human adult retina library (Genome Systems Inc.) was used to probe a Northern blot containing mRNAs from chick retinas at different developmental stages (Fig. 10A). Three AP-2 transcripts of ~1.8, 3.5, and 4 kb (indicated by the arrows) were detected after washing of the blots under moderate stringency, with the strongest signal obtained at d10. By d16, AP-2 transcript levels were significantly reduced. AP-2 transcripts were not detected at d5, while weak bands at 1.8 and 4 kb were observed at d7. The band marked by an asterisk represents residual signal from a previous hybridization and is unrelated to AP-2 mRNA.

We used a commercially available anti-human AP-2 antibody specific for AP-2α to measure AP-2 levels in the d7 and d16 nuclear extracts used for the footprinting and EMSA experiments. In agreement with the gel shift assays and the Northern blot analysis, we found considerably lower levels of AP-2α in d7 compared to d16 retinal extracts (Fig. 10B). Analysis of total cellular lysates indicate that levels of AP-2α are at least 10-fold lower in d7 retina compared to d10 retina and approximately 2-fold lower in d16 retina compared to d10 retina (data not shown). AP-2α was not detected in d5 retina.

**Mutation analysis of the AP-2 binding site.** To more directly assess the role of the *R-FABP* AP-2 binding site in proliferating retinal cells, we transfected primary d5 retinal cultures with pCAT constructs carrying mutations in the core recognition sequence for AP-2. In mutant 1 (MT1), the AP-2 sequence 5′-**GCC**GTG**GGC** (conserved residues in boldface) was mutated to GTTGTGGGC and in mutant 2 (MT2), the AP-2 site was mutated to GTTGTGTTC. The mutations were introduced into the −135-bp construct, which contains 135 bp of *R-FABP* upstream sequence. Comparison of the WT and mutant −135-bp constructs indicates that mutations in the AP-2 binding site have only a slight effect on CAT activity, decreasing levels by <2-fold (Fig. 4B). Since there are only two clear footprints in the *R-FABP* proximal regulatory region with d7 retinal extracts, we tested a −65-bp construct to determine whether inclusion of sequences between −51 bp and the AP-2 site (located from −67 to −75 bp) might increase CAT activity to the levels observed with the −135-bp construct. Again, there was only a slight increase (between 1.2- and 1.7-fold) in CAT activity in the −65-bp compared to the −51-bp construct.

We tested whether AP-2 could bind to the mutated AP-2

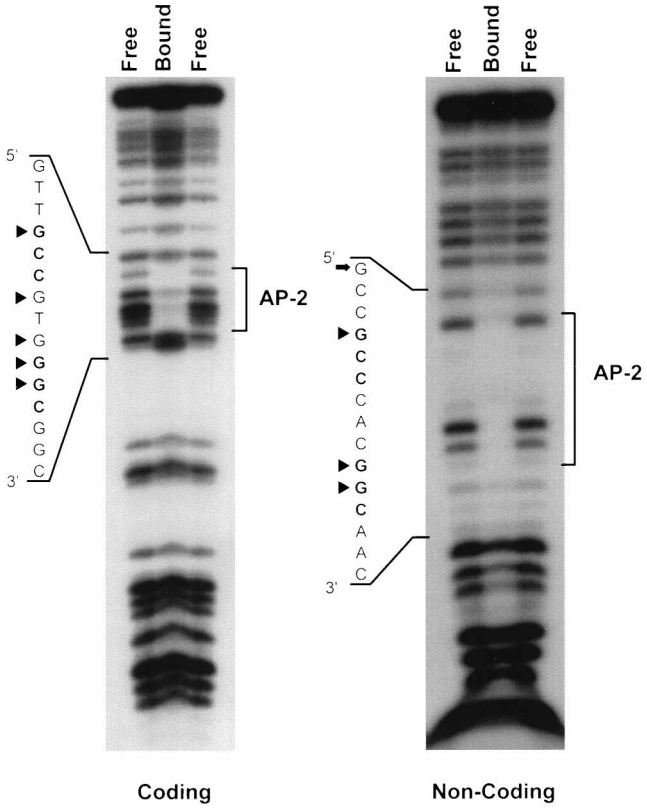


FIG. 9. Methylation interference with the DNA fragment from −52 to −90 bp (containing footprint II). EMSA was carried out with either d7 (not shown) or d16 (shown) chick retinal extract with a partially methylated singly end-labelled probe representing the coding and noncoding strands. The bands corresponding to free DNA and protein-bound DNA (major band indicated by the arrows in Fig. 7) were excised, and the DNA was eluted, cleaved with piperidine, and electrophoresed in an 8% (coding strand) or 12% (noncoding strand) denaturing polyacrylamide gel. The conserved residues in the AP-2 DNA binding site are indicated in boldface (5′-**GCC**NNN**GGC**-3′). The arrowheads indicate the G residues that are part of the AP-2 binding site in which methylation interferes with AP-2 binding. The arrow indicates the G residue in the noncoding strand that lies outside the consensus AP-2 binding site.

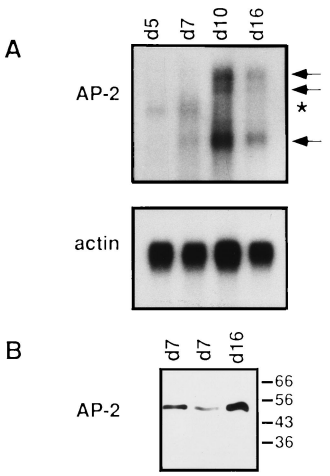


FIG. 10. Analysis of AP-2 transcript and protein levels in the chick retina at different developmental stages. (A) Poly(A)$^+$ RNA was extracted from d5, d7, d10, and d16 chick retinas. After electrophoresis, the RNA (2 μg/lane) was transferred to a nitrocellulose filter and sequentially hybridized with $^{32}$P-labelled AP-2 cDNA isolated from a human adult retina library and actin cDNA. The blot hybridized with AP-2 cDNA was washed at 45°C in 0.1× SSC–0.1% SDS. Exposure to X-ray film was 3 days for the AP-2 cDNA probe and 1 h for the actin probe. The arrows indicate the position of the AP-2 transcripts. The band marked by an asterisk represents residual signal from a previous hybridization. (B) Western blots were prepared with nuclear extracts from two different preparations of d7 retina and from d16 retina. Fifty micrograms of protein was loaded in each of the d7 lanes, and 25 μg was loaded in the d16 lane. AP-2 was detected with a commercially available anti-human AP-2 antibody that specifically recognizes AP-2α. Molecular mass standards (kilodaltons) are indicated on the side.

recognition site by EMSA. WT and mutant 1 (MT1) labelled DNA fragments from −52 to −90 bp served as probes for these experiments. The intense band indicated by the arrow in Fig. 7 is readily apparent in the presence of WT probe (Fig. 11, lanes 2 and 8) but is absent with mutant DNA as the probe (lanes 3 and 9). This band was previously shown to supershift in the presence of AP-2 antibody. Competition experiments indicate that a 50× excess of unlabelled WT DNA serves as an effective competitor for binding to this factor (lanes 4 and 10), while a 100× excess of mutant DNA fails to reduce the intensity of this band (lanes 7 and 13). Retarded bands with a higher migration rate were also observed with both the WT and mutant DNA as the probe (lanes 2, 3, 8, and 9). A reduction in the intensity of these bands was obtained when WT and mutant DNAs were used as competitors, although mutant DNA was not as effective as WT DNA (compare lanes 6, 7, 12, and 13 with lanes 4, 5, 10, and 11). It should be noted that these lower bands did not supershift in the presence of AP-2 antibody (Fig. 8). Another weak band located near the gel origin (shown not to be competed out with excess unlabelled AP-2 oligonucleotide in Fig. 7) was restricted to the lanes containing the WT probe (lanes 2 and 8). Qualitatively similar results were observed with d7 and d16 retinal extracts, although the signal intensity was considerably lower with d7 extracts.

## DISCUSSION

The retina is well characterized morphologically and physiologically. The time of appearance and location of each of the major cell types in the retina as well as the function of these cells have been described for a number of species. However, we still have a poor understanding of the nature and function of the precursor neuroectodermal cells that differentiate into the various classes of neurons and glia found in the mature retina. *R-FABP* is expressed in tissues derived from neuroectodermal cells, including brain and retina. In the retina, *R-FABP* has an expression profile that suggests a role in cell proliferation and early differentiation; i.e., *R-FABP* is expressed at elevated levels in the undifferentiated cells of the retina, and tissue maturation is accompanied by a dramatic decrease in mRNA levels (50- to 100-fold decrease from d3.5 to d19 of incubation) (24). We analyzed the regulation of the *R-FABP* gene in order to gain insight into the molecular mechanisms and transcription factors involved in controlling gene expression in the retinal neuroectodermal cells.

The 5′ flanking DNA of the chicken *R-FABP* gene has an extremely high GC content, with >80% G's and C's over 200 bp of 5′ flanking DNA, including 33 CpGs. The expression of some genes has been shown to be closely related to the methylation status of CpGs in their promoter regions (reviewed in reference 17). Nonmethylated CpG islands are generally believed to be associated with sites of transcribed genes, while CpG methylation apparently inhibits transcription. Some transcription factors which contain CpGs in their recognition sites are affected by methylation (e.g., AP-2) (14) while others (e.g., Sp1) (32) are not. DNA methylation appears to function by preventing the binding of some transcription factors and by altering chromatin structure (reviewed in reference 17). We have found no evidence of methylation in the promoter region of the *R-FABP* gene either in retina (differentiated or undifferentiated tissue) or in the adult liver where R-FABP mRNA is not detected. These results suggest that CpG methylation in the immediate upstream region of the *R-FABP* gene is not involved in the repression of *R-FABP* gene transcription, at least in the differentiated retina and liver. Similar observations have been made for the human α-globin gene, whose promoter is unmethylated not only in tissues expressing the α-globin gene but in nonexpressing tissues as well (5).

We used nuclear extracts of d7 and d16 retinas to study DNA-protein interactions in the upstream region of the *R-FABP* gene. At d7, 60% of retinal cells are proliferating (16) and R-FABP transcript levels are high (24, 26). The relatively large size of the eyes at this late proliferative stage facilitates the accumulation of the large quantities of retinal tissue re-

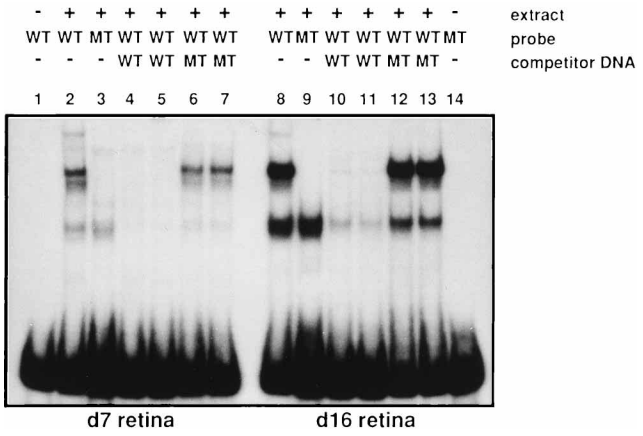


FIG. 11. Mutation of the core recognition sequence for AP-2 binding prevents DNA-protein interaction. EMSAs were carried out with WT (WT AP-2, GCCGTGGGC) and mutant (MT AP-2, GTTGTGGGC) DNA fragments from −52 to −90 bp. The $^{32}$P-labelled probes were incubated with nuclear extracts from either d7 or d16 retina in the presence or absence of WT or mutant competitor DNA. There was a 50× excess of competitor in lanes 4 (WT), 6 (MT), 10 (WT), and 12 (MT) and a 100× excess in lanes 5 (WT), 7 (MT), 11 (WT), and 13 (MT).

quired for these analyses. DNase I hypersensitivity and DNA-protein interaction studies with d7 retina suggest that the major regions responsible for transcriptional regulation of the *R-FABP* gene are located within 205 bp of the transcription initiation site. Three footprints were identified in this region with d7 retinal extracts, and four footprints were identified with d16 retinal extracts. Footprint I (−24 to −52 bp) includes a putative TATA box (TTTAAA) located 30 bp upstream of the *R-FABP* transcription start site as well as SP1 consensus sites and is required for basal transcriptional activity based on transient CAT expression in primary d5 retinal cultures. Of note, another *FABP* gene closely related to *R-FABP*, mouse *H-FABP*, also has a TTTAAA sequence located −21 to −26 bp upstream of the transcription start site (47). A subset of *FABP* genes may show a preference for this sequence, similar to what has been reported for the milk protein genes (61). A construct that includes footprint II (−63 to −80 bp) in addition to footprint I generated a four- to fivefold increase in CAT activity compared to a construct with footprint I alone. Additional 5′ flanking DNA, including footprint IV at −199 to −205 bp, resulted in a <2-fold further increase in CAT activity. Footprint III (−114 to −140 bp) is found only with d16 retinal extracts and may play a negative role in the regulation of *R-FABP* transcription.

Footprint II is of special interest because different patterns are observed with d7 (footprint from −63 to −80 bp) and d16 (−59 to −80 bp) retinal extracts, suggesting that the interaction of nuclear protein(s) with this DNA region differs in the undifferentiated and differentiated retinas. Furthermore, footprint II includes an AP-2 consensus binding site, 5′-GCCNN NGGC-3′. AP-2 is a transcription factor implicated in gene regulation during embryogenesis (57) and has been shown to be involved in the differentiation of P19 embryonal carcinoma cells along the neuroectodermal pathway by retinoic acid (43). A number of genes have been found to be regulated by AP-2, including insulin-like growth factor-binding protein 5, which is expressed in the retina (10, 15). There are at least three genes that encode members of the AP-2 family in mammals, *AP-2*α, *AP-2*β, and *AP-2*γ (39, 58). To date, only the *AP-2*α cDNA has been isolated from chicken cells (EMBL/GenBank accession no. U72992). AP-2 factors encoded by all three genes bind as dimers to the same AP-2 DNA recognition sites. These factors have similar dimerization domains but differ in their transactivation domains. AP-2α consists of two splice variants, AP-2αA and AP-2αB (9). The latter is a negative regulator of transcriptional activation by AP-2 and functions by blocking DNA binding. The AP-2 family is therefore considerably more complex than originally anticipated, suggesting a need for controlling AP-2 activity at multiple levels and in a tissue- or cell-specific manner. Gel shift assays with an AP-2 consensus oligomer as the competitor, supershift experiments with AP-2 antibody, and methylation interference experiments all indicate that a member of the AP-2 family binds to footprint II located upstream of the *R-FABP* gene. Notably, although the d16 footprint extends further than the d7 footprint, the same banding patterns are observed in the EMSA and supershift experiments with either d7 or d16 retinal extracts. Furthermore, methylation interference experiments indicate that the same nucleotides are involved in nuclear protein binding in the two tissues. Taken together, these results suggest that one or more members of the AP-2 family expressed in d7 and d16 retinas are binding to the AP-2 consensus site located upstream of the *R-FABP* gene.

One would expect a positive regulator of *R-FABP* transcription to be expressed in the undifferentiated retina when R-FABP transcript levels are highest. The absence of detectable AP-2α mRNA and protein in d5 retina and its relatively low abundance in d7 retina compared to d10 retina suggest that at least this member of the AP-2 family is not an activator of *R-FABP* transcription. The comparatively weak signal observed in the DNA-protein interaction analyses (footprinting and EMSA) with d7 versus d16 retinal extracts further indicates that overall AP-2-like activity (defined as the ability to bind to the AP-2 recognition site) is significantly higher in the more differentiated retina. Based on these observations, we propose that AP-2 (most likely AP-2α) functions as a repressor rather than an activator of transcription. In support of this hypothesis, it should be noted that a decrease in the steady-state levels of R-FABP mRNA is first observed in d10 retina (24) when AP-2α transcript and protein levels peak. Furthermore, although R-FABP mRNA is abundant in the d7 retina, only 60% of cells are in the proliferative stage. The remaining cells have already differentiated or are undergoing differentiation. It is therefore possible that the factors in d7 retina that interact with the AP-2 binding site are found exclusively in the differentiated population of cells. Because of the difficulty in obtaining sufficient retinal material at earlier developmental stages for nuclear extract preparation, this question may best be resolved by identifying the AP-2 factors expressed in the developing chick retina and determining which cell types produce these factors.

Although AP-2 is generally considered to be an activator of transcription, it has also been shown to negatively regulate the transcription of the following genes: stellate cell type 1 collagen, K3 keratin, acetylcholinesterase, prothymosin, and ornithine decarboxylase (11, 12, 22, 23). In all these cases, it was proposed that AP-2 functions as a repressor by displacing or competing with a positive transcription factor that has a binding site that overlaps with or is adjacent to the AP-2 recognition site. If AP-2 functions as a transcriptional activator of the *R-FABP* gene, transfection of a construct carrying a mutated AP-2 site into proliferating retinal cells should result in a decrease in CAT activity. If, on the other hand, AP-2 functions as a transcriptional repressor, an increase in activity would be expected only in cells that express AP-2. DNA transfection of mutant constructs in which as many as four of the six conserved AP-2 residues have been altered (5′-**GCC**NNN**GGC**-3′ to either 5′-**G**TT**C**NNN**GGC**-3′ or 5′-**G**TT**C**NNN**TTC**-3′) generates only a slight decrease in CAT activity compared to the WT construct. Gel shift experiments with the mutant AP-2 recognition site show that AP-2 can no longer bind to this site. The DNA transfection results with d5 retinal cultures are therefore consistent with AP-2 functioning as a repressor of *R-FABP* transcription, in agreement with the DNA-protein interaction experiments and the AP-2 expression profile in the developing retina. We have not yet identified the sequences that are responsible for the increase in CAT activity observed between −51 and −135 bp. A positive regulatory element may overlap with the AP-2 binding site and be partially inactivated by the mutations introduced in this region. Gel shift experiments reveal the presence of a number of bands that are not competed out by excess AP-2 oligomers with a −52- to −90-bp fragment as the probe. Alternatively, sequences upstream of footprint II may be required for optimal transcriptional activity.

The extension in footprint II seen in the d16 extract may reflect the presence of an additional factor binding to this region which is detected only under the conditions used in our footprinting assay. One major difference between the gel shift and footprinting experiments is the comparatively large size of the DNA fragment used for footprinting. More complex DNA-protein interactions may therefore be favored by the latter technique. Whether the AP-2 transcription factor(s) expressed

in d7 and d16 retinas is the same or represents different members of the family or different splice variants will be the subject of future investigations. It will also be of interest to study footprint III to see if we can identify the transcription factor that binds to this region, as it may represent a transcriptional repressor for genes expressed in the differentiating retina.

In conclusion, we have used a combination of techniques to identify the regulatory elements important for the transcription of the *R-FABP* gene in the developing retina. By DNase I hypersensitivity analysis, DNA transfection, and DNA-protein interaction assays, we have shown that strong *cis* regulatory activity is located within 200 bp of the transcription initiation site of the *R-FABP* gene. The data presented here support a role for the family of AP-2 transcriptional factors in the regulation of the *R-FABP* gene in the developing retina. The AP-2 expression profile in the retina, gel shift experiments, and DNA transfection analysis with constructs carrying mutations in the conserved residues of the AP-2 binding site all suggest that AP-2 is a repressor of *R-FABP* transcription.

## ACKNOWLEDGMENTS

We thank Sachin Katyal for his technical assistance in the methylation analysis of the *R-FABP* promoter and Brian Brady, Randy Andison, and Shauna McCooeye for their assistance in the preparation of the manuscript.

This work was supported by the Medical Research Council of Canada.

## REFERENCES

1. **Bass, N. M.** 1993. Cellular binding proteins for fatty acids and retinoids: similar or specialized functions? Mol. Cell. Biochem. **123:**191–202.
2. **Bass, N. M., D. E. R. Raghuphaty, J. A. Manning, and R. K. Ockner.** 1984. Partial purification of molecular weight 12000 fatty acid binding proteins from rat brain and their effect on synaptosomal $Na^+$-dependent amino acid uptake. Biochemistry **23:**6539–6544.
3. **Belikov, S., and L. Wieslander.** 1995. Express protocol for generating G+A sequencing ladders. Nucleic Acids Res. **23:**310.
4. **Bernier, I., and P. Jollès.** 1984. Purification and characterization of a basic 23 kDa cytosolic protein from rat brain. Biochim. Biophys. Acta **790:**174–181.
5. **Bird, A. P., M. H. Taggart, R. D. Nicholls, and D. R. Higgs.** 1987. Non-methylated CpG-rich islands at the human alpha-globin locus: implications for evolution of the alpha-globin pseudogene. EMBO J. **6:**999–1004.
6. **Börchers, T., C. Unterberg, H. Rüdel, H. Robenek, and F. Spener.** 1989. Subcellular distribution of cardiac fatty acid-binding protein in bovine heart muscle and quantitation with an enzyme-linked immunosorbent assay. Biochim. Biophys. Acta **1002:**54–61.
7. **Bordewick, U., M. Hesse, T. Börchers, H. Robenek, and F. Spener.** 1989. Compartmentation of hepatic fatty-acid-binding protein in liver cells and its effect on microsomal phosphatidic acid. Biol. Chem. Hoppe-Seyler **370:**229–238.
8. **Buelt, M. K., L. L. Shekels, B. W. Jarvis, and D. A. Bernlohr.** 1991. In vitro phosphorylation of the adipocyte lipid-binding protein (p15) by the insulin receptor. J. Biol. Chem. **265:**12266–12271.
9. **Buettner, R., P. Kannan, A. Imhof, R. Bauer, S. O. Yim, R. Glockshuber, M. W. Van Dyke, and M. A. Tainsky.** 1993. An alternatively spliced mRNA from the AP-2 gene encodes a negative regulator of transcriptional activation by AP-2. Mol. Cell. Biol. **13:**4174–4185.
10. **Burren, C. P., J. L. Berka, S. R. Edmondson, G. A. Werther, and J. A. Batch.** 1996. Localization of mRNAs for insulin-like growth factor-I (IGF-I), IGF-I receptor, and IGF binding proteins in rat eye. Investig. Ophthalmol. Vis. Sci. **37:**1459–1468.
11. **Chen, A., D. W. A. Beno, and B. H. Davis.** 1996. Suppression of stellate cell type I collagen gene expression involves AP-2 transmodulation of nuclear factor-1-dependent gene transcription. J. Biol. Chem. **271:**25994–25998.
12. **Chen, T.-T., R.-L. Wu, F. Castro-Munozledo, and T.-T. Sun.** 1997. Regulation of K3 keratin gene transcription by Sp1 and AP-2 in differentiating rabbit corneal epithelial cells. Mol. Cell. Biol. **17:**3056–3064.
13. **Clark, S. J., J. Harrison, C. L. Paul, and M. Frommer.** 1994. High sensitivity mapping of methylated cytosines. Nucleic Acids Res. **22:**2990–2997.
14. **Comb, M., and H. W. Goodman.** 1990. CpG methylation inhibits proenkephalin gene expression and binding of the transcription factor AP-2. Nucleic Acids Res. **18:**3975–3982.
15. **Duan, C., and D. R. Clemmons.** 1995. Transcription factor AP-2 regulates human insulin-like growth factor binding protein-5 gene expression. J. Biol. Chem. **270:**24844–24851.
16. **Dütting, D., A. Gierer, and G. Hansmann.** 1983. Self-renewal of stem cells and differentiation of nerve cells in the developing chick retina. Dev. Brain Res. **10:**21–32.
17. **Eden, S., and H. Cedar.** 1994. Role of DNA methylation in the regulation of transcription. Curr. Opin. Genet. Dev. **4:**255–259.
18. **Feng, L., M. E. Hatten, and N. Heintz.** 1994. Brain lipid-binding protein (BLBP): a novel signaling system in the developing mammalian CNS. Neuron **12:**895–908.
19. **Feng, L., and N. Heintz.** 1995. Differentiating neurons activate transcription of the brain lipid-binding protein gene in radial glia through a novel regulatory element. Development **121:**1719–1730.
20. **Frommer, M., L. E. McDonald, D. S. Millar, C. M. Collis, F. Watt, G. W. Grigg, P. L. Molloy, and C. L. Paul.** 1992. A genomic sequencing protocol that yields a positive display of 5-methylcytosine residues in individual DNA strands. Proc. Natl. Acad. Sci. USA **89:**1827–1831.
21. **Garabedian, M. J., J. LaBaer, W.-H. Liu, and J. R. Thomas.** 1993. Analysis of protein-DNA interactions, p. 243–291. *In* B. D. Hames and S. J. Higgins (ed.), Gene transcription: a practical approach. IRL Press, Oxford, United Kingdom.
22. **Gaubatz, S., A. Imhof, R. Dosch, O. Werner, P. Mitchell, R. Buettner, and M. Eilers.** 1995. Transcriptional activation by Myc is under negative control by the transcription factor AP-2. EMBO J. **14:**1508–1519.
23. **Getman, D. K., A. Mutero, K. Inoue, and P. Taylor.** 1995. Transcription factor repression and activation of the human acetylcholinesterase gene. J. Biol. Chem. **270:**23511–23519.
24. **Godbout, R.** 1993. Identification and characterization of transcripts present at elevated levels in the undifferentiated chick retina. Exp. Eye Res. **56:**95–106.
25. **Godbout, R., R. Ingram, and S. M. Tilghman.** 1986. Multiple regulatory elements in the intergenic region between the α-fetoprotein and albumin genes. Mol. Cell. Biol. **6:**477–487.
26. **Godbout, R., H. Marusyk, D. Bisgrove, L. Dabbagh, and S. Poppema.** 1995. Localization of a fatty acid binding protein and its transcript in the developing chick retina. Exp. Eye Res. **60:**645–657.
27. **Godbout, R., and S. M. Tilghman.** 1988. Configuration of the α-fetoprotein regulatory domain during development. Genes Dev. **2:**949–956.
28. **Gorski, K. M., M. Carneiro, and U. Schibler.** 1986. Tissue-specific in vitro transcription from the mouse abumin promoter. Cell **47:**767–776.
29. **Graham, F. L., and A. J. Van der Eb.** 1973. A new technique for the assay of infectivity of human adenovirus 5 DNA. Virology **52:**456–467.
30. **Gross, D. S., and W. T. Garrard.** 1988. Nuclease hypersensitivity sites in chromatin. Annu. Rev. Biochem. **57:**159–197.
31. **Hirt, B.** 1967. Selective extraction of polyoma DNA from infected mouse cultures. J. Mol. Biol. **26:**365–369.
32. **Holler, M., G. Westin, J. Jiricny, and W. Schaffner.** 1988. Sp1 transcription factor binds DNA and activates transcription even when the binding site is CpG methylated. Genes Dev. **2:**1127–1135.
33. **Holton, T. A., and M. W. Graham.** 1991. A simple and efficient method for direct cloning of PCR products using ddT-tailed vectors. Nucleic Acids Res. **19:**1156.
34. **Jones, K. A., K. R. Yamamoto, and R. Tjian.** 1985. Two distinct transcription factors bind to the HSV thymidine kinase promoter in vitro. Cell **42:**559–572.
35. **Keler, T., C. S. Barker, and S. Sorof.** 1992. Specific growth stimulation by linoleic acid in hepatoma cell lines transfected with the target protein of a liver carcinogen. Proc. Natl. Acad. Sci. USA **89:**4830–4834.
36. **Khan, S., and S. Sorof.** 1994. Liver fatty acid-binding protein: specific mediator of the mitogenesis induced by two classes of carcinogenic peroxisome proliferators. Proc. Natl. Acad. Sci. USA **91:**848–852.
37. **Kurtz, A., A. Zimmer, F. Schnütgen, G. Brüning, F. Spener, and T. Müller.** 1994. The expression pattern of a novel gene encoding brain-fatty acid binding protein correlates with neuronal and glial cell development. Development **120:**2637–2649.
38. **Meunier-Durmort, C., H. Poirier, I. Niot, C. Forest, and P. Besnard.** 1996. Up-regulation of the expression of the gene for liver fatty acid-binding protein by long-chain fatty acids. Biochem. J. **319:**483–487.
39. **Moser, M., A. Imhof, A. Pscherer, R. Bauer, W. Amselgruber, F. Sinowatz, F. Hofstädter, R. Schüle, and R. Buettner.** 1995. Cloning and characterization of a second AP-2 transcription factor: AP-2 beta. Development **121:**2779–2788.
40. **Ngô, V., D. Gourdji, and J.-N. Laverrière.** 1996. Site-specific methylation of the rat prolactin and growth hormone promoters correlates with gene expression. Mol. Cell. Biol. **16:**3245–3254.
41. **Nielsen, S. U., and F. Spener.** 1993. Fatty acid binding protein from rat heart is phosphorylated on Tyr19 in response to insulin stimulation. J. Lipid Res. **34:**1355–1366.
42. **O'Brien, R. M., E. L. Noisin, A. Suwanichkul, T. Yamasaki, P. C. Lucas, J.-C. Wang, D. R. Powell, and D. K. Granner.** 1995. Hepatic nuclear factor 3- and hormone-regulated expression of phosphoenolpyruvate carboxykinase and insulin-like growth factor-binding protein 1 genes. Mol. Cell. Biol. **15:**1747–1758.
43. **Philipp, J., P. J. Mitchell, U. Malipiero, and A. Fontana.** 1994. Cell type-specific regulation of expression of transcription factor AP-2 in neuroecto-

dermal cells. Dev. Biol. **165:**602–614.
44. **Prada, C., J. Puga, L. Pérez-Méndez, R. López, and G. Ramirez.** 1991. Spatial and temporal patterns of neurogenesis in the chick retina. Eur. J. Neurosci. **3:**559–569.
45. **Sambrook, J., E. F. Fritsch, and T. Maniatis.** 1989. Molecular cloning: a laboratory manual, 2nd ed. Cold Spring Harbor Laboratory, Cold Spring Harbor, N.Y.
46. **Specht, B., N. Bartetzko, C. Hohoff, H. Kuhl, R. Franke, T. Börchers, and F. Spener.** 1996. Mammary derived growth inhibitor is not a distinct protein but a mix of heart-type and adipocyte-type fatty acid-binding protein. J. Biol. Chem. **271:**19943–19949.
47. **Treuner, M., C. A. Kozak, D. Gallahan, R. Grosse, and T. Müller.** 1994. Cloning and characterization of the mouse gene encoding mammary-derived growth inhibitor/heart-fatty acid-binding protein. Gene **147:**237–242.
48. **Tsukiyama, T., P. B. Becker, and C. Wu.** 1994. ATP-dependent nucleosome disruption at a heat-shock promoter mediated by binding of GAGA transcription factor. Nature **367:**525–532.
49. **Turner, D. L., and C. L. Cepko.** 1987. A common progenitor for neurons and glia persists in rat retinas late in development. Nature **328:**131–136.
50. **Turner, D. L., E. Y. Snyder, and C. L. Cepko.** 1990. Lineage-independent determination of cell type in the embryonic mouse retina. Neuron **4:**833–845.
51. **Veerkamp, J. H., and R. G. H. J. Maatman.** 1995. Cytoplasmic fatty acid-binding proteins: their structure and genes. Prog. Lipid Res. **34:**17–52.
52. **Wadzinski, B. E., W. H. Wheat, S. Jaspers, L. F. Peruski, Jr., R. L. Lickteig, G. L. Johnson, and D. J. Klemm.** 1993. Nuclear protein phosphatase 2A dephosphorylates protein kinase A-phosphorylated CREB and regulates CREB transcriptional stimulation. Mol. Cell. Biol. **13:**2822–2834.
53. **Wetts, R., and S. E. Fraser.** 1988. Multipotent precursors can give rise to all major cell types of the frog retina. Science **239:**1142–1145.
54. **Wharton, K. A., B. Yedvobnick, V. G. Finnerty, and S. Artavanis-Tsakonas.** 1985. Opa: a novel family of transcribed repeats shared by the Notch locus and other developmentally regulated loci in D. melanogaster. Cell **40:**55–62.
55. **Williams, R. W., and D. Goldowitz.** 1992. Lineage versus environment in embryonic retina: a revisionist perspective. Trends Neurosci. **15:**368–373.
56. **Williams, R. W., and D. Goldowitz.** 1992. Structure of clonal and polyclonal cell arrays in chimeric mouse retina. Proc. Natl. Acad. Sci. USA **89:**1184–1188.
57. **Williams, T., and R. Tjian.** 1991. Analysis of the DNA-binding and activation properties of the human transcription factor AP-2. Genes Dev. **5:**670–682.
58. **Williamson, J. A., J. M. Bosher, A. Skinner, D. Sheer, T. Williams, and H. C. Hurst.** 1996. Chromosomal mapping of the human and mouse homologues of two new members of the AP-2 family of transcription factors. Genomics **35:**262–264.
59. **Wu, C.** 1980. The 5′ ends of Drosophilia heat shock genes in chromatin are hypersensitive to DNase I. Nature **286:**854–860.
60. **Yang, Y., E. Spitzer, N. Kenney, W. Zschiesche, M. Li, A. Kromminga, T. Müller, F. Spener, A. Lezius, J. H. Veerkamp, G. H. Smith, D. S. Salomon, and R. Grosse.** 1994. Members of the fatty acid binding protein family are differentiation factors for the mammary gland. J. Cell Biol. **127:**1097–1109.
61. **Yoshimura, M., and T. Oka.** 1989. Isolation and structural analysis of the mouse-casein gene. Gene **78:**267–275.